



**Enhancement of electrocatalytic abilities for reducing carbon dioxide: Functionalization with a redox-active ligand-coordinated metal complex**

Journal:	<i>Dalton Transactions</i>
Manuscript ID	DT-COM-06-2018-002288.R1
Article Type:	Communication
Date Submitted by the Author:	04-Jul-2018
Complete List of Authors:	Habib, Ahsan; Tohoku University, Chemistry Breedlove, Brian; Tohoku University, Chemistry Piangrawee, Santivongskul; Tohoku University Mian, Mohammad Rasel; Tohoku University, Chemistry Fetoh, Ahmed; Mansoura University, Chemistry Cosquer, Goulven; Tohoku University, Chemistry Yamashita, Masahiro; Tohoku University, Chemistry



Journal Name

COMMUNICATION

## Enhancement of electrocatalytic abilities for reducing carbon dioxide: Functionalization with a redox-active ligand-coordinated metal complex

Received 00th January 20xx,  
Accepted 00th January 20xx

DOI: 10.1039/x0xx00000x

www.rsc.org/

Habib Md. Ahsan,<sup>a</sup> Brian K. Breedlove,<sup>\*a</sup> Santivongskul Piangrawee,<sup>a</sup> Mohammad Rasel Mian,<sup>a</sup>  
Ahmed Fetoh,<sup>b</sup> Goulven Cosquer,<sup>ad</sup> and Masahiro Yamashita<sup>acde</sup>

**A binary system consisting of a ditopic planar pseudo-pincer ligand (qlca = quinoline-2-carbaldehyde (pyridine-2-carbonyl) hydrazone) coordinated to two metal centres affording  $\{Ru(bpy)_2\}(\mu\text{-qlca})NiCl_2\}Cl \cdot 4H_2O \cdot CH_3OH$  (2) (bpy = 2,2'-bipyridine) is reported. The  $Ni^{2+}$  moiety acts as the electrocatalytic active site for  $CO_2$  reduction to CO. The turnover frequency (TOF) increased from  $0.83\ s^{-1}$  for  $[Ni(qlca)Cl_2]$  (3) to  $120\ s^{-1}$  for 2, and the overpotential is 350 mV less than that for 3 due to the electronic influence of the  $\{Ru(bpy)_2\}^{2+}$  moiety on the catalytic active site.**

Conversion of  $CO_2$  to low-carbon fuels is an excellent way to meet the increasing demand for energy while lowering the impact of  $CO_2$ , a primary greenhouse gas, on the environment.<sup>1–5</sup> Although several approaches have been used to develop efficient and selective catalysts for  $CO_2$  reduction, challenges remain. A key challenge is the development of  $CO_2$ -selective homogeneous electrocatalysts, which are highly active and selective for the specific catalytic process at low overpotential. State-of-the-art  $CO_2$  reduction electrocatalysts, such as Mn, Co and Fe complexes, have high catalytic performance at very low overpotentials.<sup>6–15</sup> In the case of a Mn complex,  $Mg^{2+}$  cation acting as a Lewis acid causes an increase in the rate of "slow catalysis" regime at a low overpotential.<sup>6</sup> However, disproportionation of  $CO_2$  to CO and  $CO_3^{2-}$  occurs, lowering the Faradaic efficiency for CO. On the other hand, Savéant and coworkers have shown that cations improve the

electrocatalytic activity.<sup>9</sup> Robert et al. have reported that an electrogenerated porphyrin Fe(0) complex with electron-withdrawing triethylanilinium groups on the ortho position of the phenyl rings of the porphyrin ligand has a turnover frequency (TOF) of up to  $10^6\ s^{-1}$  at an overpotential of 0.22 V.<sup>8</sup> Another way to improve electrocatalytic abilities is to utilize redox-active ligands<sup>11,16–25</sup> because they can store electrons in the structure, which can be utilized for  $CO_2$  activation, helping to improve the efficiently for reduction  $CO_2$  to CO.<sup>22,23,26</sup>

Metal complexes with pincer ligands have been shown to be promising electrocatalysts for the reduction of  $CO_2$  to useful chemicals,<sup>27–30</sup> and penta-coordinated pincer-type nickel complexes have been studied for  $CO_2$  reduction because they have a vacant site for  $CO_2$  activation.<sup>31,32</sup> However, pincer-type electrocatalysts suffer from low selectivity and high overpotentials. In our previous study on  $CO_2$  reduction, we attached redox-active metal complexes to electrocatalysts to improve their electrocatalytic abilities.<sup>33,34</sup> Since ruthenium polypyridyl moieties, like  $\{Ru(bpy)_2\}^{2+}$ , have rich redox properties and have a cationic metal ion,<sup>35</sup> we have recently started exploring their use to enhance catalytic abilities. In this work, we used a ditopic planar redox-active pseudo-pincer ligand, quinolone-2-carbaldehyde (pyridine-2-carbonyl) hydrazone (qlca), to tether a redox-active metal complex,  $\{Ru(bpy)_2\}^{2+}$ , to electrocatalyst moiety, which allows for more electron density near the active site. Since the redox-active metal complex and electrocatalytic centre are tethered in close proximity to each other, we believed that the electrocatalytic ability towards the conversion of  $CO_2$  to CO would be improved while maintaining the selectivity and decreasing the overpotential.

The synthesis and structural diagrams of the complexes are shown in Scheme 1, and detailed synthetic procedures are provided in the Electronic Supplementary Information (ESI). The bridging ligand qlca was prepared following a previously reported procedure.<sup>35</sup>  $[Ru(bpy)_2(qlca)Cl]$  (1) was synthesized

<sup>a</sup> Department of Chemistry, Graduate School of Science, Tohoku University, 6-3 Aza-Aoba, Aramaki, Sendai 980-8578, Japan. E-mail: [breedlove@m.tohoku.ac.jp](mailto:breedlove@m.tohoku.ac.jp)

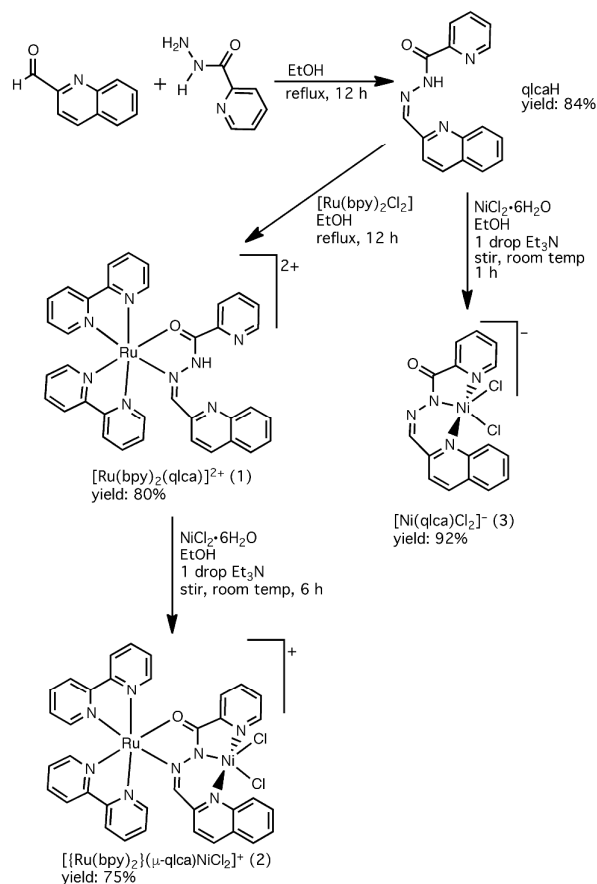
<sup>b</sup> Department of Chemistry, Faculty of Science, Mansoura University, Mansoura, Egypt.

<sup>c</sup> WPI Research Center, Advanced Institute for Materials Research, Tohoku University, 2-1-1 Katahira, Aoba-ku, Sendai 980-8577, Japan

<sup>d</sup> Core Research for Evolutional Science and Technology (CREST), Japan Science and Technology (JST), 4-1-8 Kawaguchi, Saitama 332-0012

<sup>e</sup> School of Materials and Engineering, Nankai University, Tianjin 300350, China  
Electronic Supplementary Information (ESI) available: [Procedures for synthetic, spectroscopic and electrochemical experiments. CCDC 1815967]. See DOI: 10.1039/x0xx00000x

by mixing  $\text{cis-[Ru(bpy)}_2\text{Cl}_2\text{]}$  and  $\text{qlca}$  in ethanolic solution (see ESI).



**3** was obtained from the reaction of  $\text{NiCl}_2 \cdot 6\text{H}_2\text{O}$  and  $\text{qlca}$  in ethanol in the presence of trimethylamine. **2** was obtained by reacting  $\text{NiCl}_2 \cdot 6\text{H}_2\text{O}$  and **1** in an ethanolic solution. Deep-red plate-like single crystals of **2** were obtained after 3–4 days.

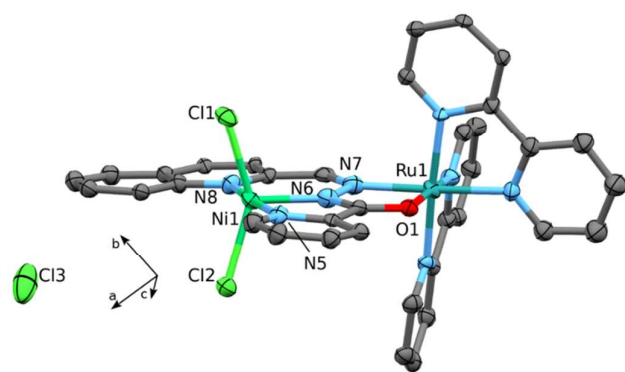


**Fig. 1** ORTEP diagram of **2** at 50% probability. Hydrogen atoms and solvent molecules are omitted for clarity. Selected bond distances (Å): Ni1–N5 = 2.07(2); Ni1–N6 = 2.01(2); Ni1–Cl1 = 2.362(6); Ni1–Cl2 = 2.333(6); N6–N7 = 1.39(2); Ru1–N7 = 2.04(2); Ru1–O1 = 2.07(1); Ru1–N1 = 2.11(2); Ru1–N2 = 2.09(1); Ru–N3 = 2.09(2); Ru1–N4 = 2.03(2); C26–O1 = 1.28(2). Selected bond angles (°): Cl1–Ni1–Cl2 = 147.1(2); N5–Ni1–Cl1 = 89.1(5); N5–Ni1–Cl2 = 92.0(5); N5–Ni1–N6 = 80.5(6); N5–Ni1–N8 = 174.0(6); N1–Ru1–N7 = 172.6(6); O1–Ru1–N7 = 79.3(3).

An ORTEP diagram of **2** is shown in Fig. 1, and the crystal data are summarized in Table S1. **2** crystallizes in the monoclinic space group  $P2_1$ . The asymmetric unit is composed of two  $\text{bpy}$  ligands coordinated to a  $\text{Ru}^{\text{II}}$  ion, one  $\text{Ni}^{\text{II}}$  ion coordinated by two  $\text{Cl}^-$  ions, one  $\text{qlca}$  ligand bridging the  $\text{Ru}^{\text{II}}$  and  $\text{Ni}^{\text{II}}$  ions and a  $\text{Cl}^-$  ion as a counter ion. Similar to the structure reported by A. Mori *et al.*, the hydrazone group of the  $\text{qlca}$  ligand is deprotonated.<sup>36</sup> Atoms N8, N6 and N5 of the  $\text{qlca}$  ligand coordinate to the  $\text{Ni}^{\text{II}}$  ion in a tridentate mode. The  $\text{Ru}^{\text{II}}$  ion in the  $\{\text{Ru}(\text{bpy})_2\}^{2+}$  moiety adopts an octahedral geometry and is coordinated by atoms N7 and O1 of  $\text{qlca}$  in a bidentate mode. The O1–C26, C26–N6 and N6–N7, N7–C27 bond lengths were determined to be 1.28(3), 1.36(3), 1.38(3), and 1.31(3) Å, respectively, suggesting that the negative charge of the ligand is delocalized in this region.<sup>37,38</sup> In ESI mass spectra (Fig. S2), the molecular ion peak was observed at 817  $m/z$ , which corresponds to  $[\{\text{Ru}(\text{bpy})_2\}(\text{qlca})\text{NiCl}_2]^+$ . There are methanol and four water molecules per asymmetric unit at 93 K. Elemental analysis of desolvated **2** was consistent with the calculated value for  $[\{\text{Ru}(\text{bpy})_2\}(\mu\text{-qlca})\text{NiCl}_2]\text{Cl}$ .

Electrochemical properties of **2** and **3** were investigated by using

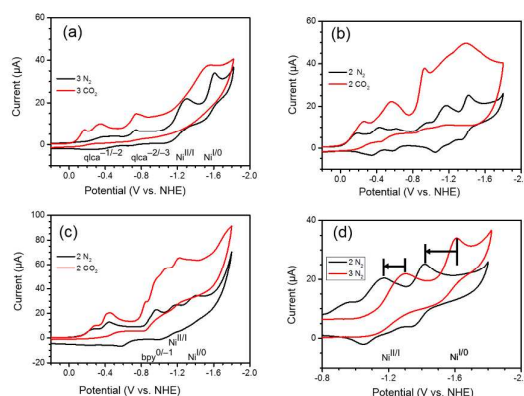


**Fig. 2.** (a) Cyclic voltammograms (CVs) of **3** (0.5 mM) in 5%  $\text{H}_2\text{O}$  and  $\text{CH}_3\text{CN}$  solution mixture under  $\text{N}_2$  (black) and  $\text{CO}_2$  saturated (red), (b) **2** (0.5 mM) in  $\text{CH}_3\text{CN}$  solution under  $\text{N}_2$  (black) and  $\text{CO}_2$  (red), and (c) **2** (0.5 mM) in 5%  $\text{H}_2\text{O}$  and  $\text{CH}_3\text{CN}$  solution mixture under  $\text{N}_2$  (black) and  $\text{CO}_2$  (red). (d) Shift in the  $\text{Ni}^{\text{II/I}}$  and  $\text{Ni}^{\text{I/0}}$  potentials in the CVs of **2** (black) and **3** (red) under  $\text{N}_2$  due to an inductive effect from the  $\{\text{Ru}(\text{bpy})_2\}^{2+}$  moiety. Scan rate for all CVs was 0.1 V/s, and 0.1M  $\text{TBAPF}_6$  was used as an electrolyte. A glassy carbon electrode was as the working electrode.

cyclic voltammetry (see ESI for details). Cyclic voltammograms (CVs) of **3** were acquired in 5:95 (v/v) mixture of  $\text{H}_2\text{O}$  and  $\text{CH}_3\text{CN}$  containing 0.1 M tetrabutylammonium hexafluorophosphate ( $\text{TBAPF}_6$ ) saturated with  $\text{N}_2$  and  $\text{CO}_2$  and are shown in Fig. 2a. The broad wave at  $-0.40$  V and wave at  $-0.72$  V vs. NHE were assigned to be due to the first and second reduction of the  $\text{qlca}$  ligand, respectively. The waves at  $-1.30$  V and  $-1.61$  V vs. NHE were assigned to  $\text{Ni}^{\text{II/I}}$  and  $\text{Ni}^{\text{I/0}}$  couples, respectively. Under  $\text{CO}_2$ , the catalytic current slightly increased, indicating weak electrocatalysis.

For **2** (Fig. 2b), in dry  $\text{CH}_3\text{CN}$  solution, the waves at  $-0.18$  V (under  $\text{CO}_2$  same wave appeared for **3**) and  $-0.62$  V vs. NHE were assigned to the first and second reduction of the  $\text{qlca}$  ligand, and those at  $-0.45$  and  $-0.95$  V vs. NHE were assigned to first and second reduction of  $\text{bpy}$  ligands, respectively. The waves at  $-1.20$  V and  $-1.42$  V vs. NHE assigned to the  $\text{Ni}^{\text{II/I}}$  and  $\text{Ni}^{\text{I/0}}$  couples, respectively.

The waves for the Ni<sup>II/I</sup> and Ni<sup>I/0</sup> couples were at less negative potentials than those for **3** (Fig. 2d) because of cationic effects of the Ru<sup>2+</sup> center. A similar behavior has been observed when Ca<sup>2+</sup> or Na<sup>+</sup> is added to other electrocatalytic systems.<sup>36</sup> The current was enhanced, indicating the reduction of CO<sub>2</sub>, and the enhancement was much higher than that using **3**, showing the electronic influence of {Ru(bpy)<sub>2</sub>}<sup>2+</sup> moiety on the electrocatalytic center. The CVs of **2** in 5:95 (v/v) mixture of H<sub>2</sub>O and CH<sub>3</sub>CN (v/v) and found that the reduction wave for the Ni<sup>II/I</sup> couple decreased at -1.17 V and the Ni<sup>I/0</sup> couple at -1.40 V vs. NHE (Fig. 2c). Under CO<sub>2</sub>, the increase in the catalytic current was larger than that using **3**, and the catalytic potential was shifted positively. Although the overall negative charge of **3** causes the Ni<sup>II/I</sup> reduction potential to be more negative and makes a direct comparison of the CVs of **2** and **3** difficult, it is clear that attaching a cationic redox-active {Ru(bpy)<sub>2</sub>}<sup>2+</sup> moiety causes a positive shift in the Ni<sup>II/I</sup> potential as well as the catalytic potential (Fig. 2d), reducing the overpotential needed to reduce CO<sub>2</sub>.

Control potential electrolysis (CPE) experiments were performed to determine the catalytic abilities of **2** and **3** for CO<sub>2</sub> reduction. CPE was performed for 30 min at potentials necessary for electrocatalytic activity. Samples of the headspace were obtained by using a gas-tight syringe during electrocatalysis and analyzed by using gas chromatography-mass spectrometry (GC-mass). In the gas phase, the main product in both cases was CO. The Faradaic efficiencies for CO were determined to be 61% for **3** and 82% for **2** in 5:95 (v/v) H<sub>2</sub>O/CH<sub>3</sub>CN. The turnover frequencies (TOFs) were determined from CPE data at -1.55 V for **3** and -1.20 V vs. NHE for **2** to be 0.83 and 120 s<sup>-1</sup>, respectively, by using Eq. 1, which McCrory *et al.*<sup>22</sup> modified from equations introduced by Savéant and coworkers.<sup>14,39</sup>

$$TOF = \frac{(i_{el})^2 (1 + \exp[\frac{F}{RT}(E_{app} - E_{1/2}])}{F^2 A^2 D [cat]^2} \quad \text{Eq. 1}$$

where  $i_{el}$  is the average current of CPE for CO generation (A),  $F$  is Faraday's constant (96500 C mol<sup>-1</sup>),  $R$  is the universal gas constant (8.31 J K<sup>-1</sup> mol<sup>-1</sup>),  $T$  is the temperature (298 K),  $E_{app}$  is the applied potential during CPE,  $E_{1/2}$  is the standard redox potential of the catalyst,  $A$  is the surface area of working electrode (0.196 cm<sup>2</sup>),  $D$  is the diffusion coefficient for catalyst and  $[cat]$  is the concentration of catalyst in solution. The overpotentials using **2** and **3** are 480 and 830 mV. In other words, {Ru(bpy)<sub>2</sub>}<sup>2+</sup> lowers catalytic potential. However, in this case, the Faradaic efficiency was maintained. This is different than when Mg<sup>2+</sup> was used as disproportionation occurred.<sup>6</sup> The TOF value for **2** is higher than those estimated for reported pincer (carbene-pyridine-carbene) and pincer-type (NNN) bis(ketimino)pyridine nickel complexes (90 s<sup>-1</sup> and 2.9 s<sup>-1</sup>, respectively).<sup>31,32</sup> The differences in the electrocatalytic parameters for **2** and **3** as well as other pincer-type Ni<sup>II</sup> complexes clearly show that tethering a redox-active cationic moiety to the electrocatalyst is advantageous for not only decreasing the overpotential but also improving TOF while maintaining or improving the efficiency of the electrocatalytic system.

In summary, we designed a new binary system consisting of a redox-active metal complex {Ru(bpy)<sub>2</sub>}<sup>2+</sup> and a metal centre with an electrocatalytic active site (Ni<sup>2+</sup>) connected via a ditopic planar redox-active pseudo pincer-type ligand. The electrocatalytic abilities of **2** were improved due to the electronic influence of redox-active {Ru(bpy)<sub>2</sub>}<sup>2+</sup> moiety. TOF increased from 0.83 s<sup>-1</sup> for **3** to 120 s<sup>-1</sup> for **2**. The overpotential for **2** is 350 mV less than **3**. These results show the advantages of tethering a redox-active moiety to an electrocatalyst, and we are currently applying this approach to other electrocatalysis systems.

## Conflicts of interest

There are no conflicts to declare.

## Acknowledgements

This work was partially supported by CREST (JPMJCR12L3), JST

## References

- M. Aresta and A. Dibenedetto, *Dalton Trans.*, 2007, 2975–2992.
- H. Takeda, C. Cometto and O. Ishitani, M. Robert, *ACS. Catal.*, 2017, **7**, 70–88.
- J. Qiao, Y. Liu, F. Hong and J. Zhang, *Chem. Soc. Rev.*, 2014, **45**, 631–675.
- J. Albo, M. A. Guerra, P. Castano and A. Irabien, *Green Chem.*, 2015, **17**, 2304–2324.
- K. L. Materna, R. H. Crabtree and G. W. Brudvig, *Chem. Soc. Rev.*, 2017, **46**, 6099–6110.
- M. D. Sampson and C. P. Kubiak, *J. Am. Chem. Soc.*, 2017, **138**, 1386–1396.
- C. Cometto, L. Chen, P. K. Lo, Z. Guo, K. C. Lau, E. A. Mallart, A. Fave, T. C. Lau and M. Robert, *ACS Catal.*, 2018, **8**, 3411–3417.
- I. Azcarate, C. Costentin, M. Robert and J. M. Saveant, *J. Am. Chem. Soc.*, 2016, **138**, 16639–16644.
- M. Hammouche, D. Lexa, M. Momenteau and J. M. Saveant, *J. Am. Chem. Soc.*, 1991, **113**, 8455–8466.
- K. T. Ngo, M. McKinnon, B. Mahanti, R. Narayanan, D. C. Grills and M. Z. Ertem, J. Rochford, *J. Am. Chem. Soc.*, 2017, **139**, 2604–2618.
- C. W. Machan, M. D. Sampson and C. P. Kubiak, *J. Am. Chem. Soc.*, 2015, **137**, 8564–8571.
- M. L. Clark, K. A. Grice, C. E. Moore, A. Rheingold and C. P. Kubiak, *Chem. Sci.*, 2014, **5**, 1894–1900.
- G. Neri, I. M. Aldous, J. J. Walsh, L. J. Hardwick and A. J. Cowan, *Chem. Sci.*, 2016, **7**, 1521–1526.
- C. Costentin, S. Drouet, M. Robert and J. M. Saveant, *Science*, 2012, **338**, 90–94.
- C. W. Machan, S. A. Chabolla and C. P. Kubiak, *organometallics*, 2015, **34**, 4678–4683.
- M. Bourrez, F. Molton, S. C. Noblat and A. Deronzier, *Angew. Chem. Int. Ed.*, 2011, **50**, 9903–9906.
- E. Fujita and J. T. Muckerman, *Inorg. Chem.*, 2004, **43**, 7636–7647.
- J. A. Therrien, M. O. Wolf and B. O. Patrick, *Inorg. Chem.*, 2015, **54**, 11721–11732.

- 19 J. M. Smieja and C. P. Kubiak, *Inorg. Chem.*, 2010, **49**, 9283–9289.
- 20 J. A. Keith, K. A. Grices, C. P. Kubiak and E. A. Carter, *J. Am. Chem. Soc.*, 2013, **135**, 15823–15829.
- 21 Z. Chen, C. Chen, D. R. Weinberg, P. Kang, J. J. Concepcion, D. P. Harrison, M. S. Brookhart and T. J. Meyer, *Chem. Commun.*, 2011, **47**, 12607–12609.
- 22 W. Nie, C. C. L. McCrory, *Chem. Commun.*, 2018, **54**, 1579–1582.
- 23 D. C. Lacy, C. C. L. McCrory and J. C. Peters, *Inorg. Chem.*, 2014, **53**, 4980–4988.
- 24 X. Su, K. M. McCardle, J. A. Panetier and J. W. Jurss, *Chem. Commun.*, 2018, **54**, 3351–3354.
- 25 F. W. Liu, J. Bi, Y. Sun, S. Lue and P. Kang, *ChemSusChem*, 2018, **11**, 1–9.
- 26 L. Chen, Z. Guo, X. G. Wei, C. Gallenkamp, J. Bonin, E. A. Mallart, K. C. Lau, T. C. Lau and M. Robert, *J. Am. Chem. Soc.*, 2015, **137**, 10918–10921.
- 27 T. J. Schmeier, G. E. Dobreiner, R. H. Crabtree and N. Hazari, *J. Am. Chem. Soc.*, 2011, **133**, 9274–9277.
- 28 R. Langer, Y. D. Posner, G. Leitus, L. J. W. Shimon, Y. B. David and D. Milstein, *Angew. Chem. Int. Ed.*, 2011, **50**, 9948–9952.
- 29 G. A. Andrade, J. L. DiMiglio, E. T. Guardino, G. P.A. Yap and J. Rosenthal, *Polyhedron*, 2017, **135**, 134–143.
- 30 W.H. Wang, Y. Himeda, J. T. Muckerman, G. F. Manbeck and E. Fujita, *Chem. Rev.*, 2015, **115**, 12936–12973.
- 31 M. Sheng, N. Jiang, S. Gustafson, B. You, D. H. Ess and Y. Sun, *Dalton Trans.*, 2015, **44**, 16247–16250.
- 32 R. Narayanan, M. Mckinnon, B. R. Reed, K. T. Ngo, S. Groysman and J. Rochford, *Dalton Trans.*, 2016, **45**, 15285–15289.
- 33 B. K. Breedlove, D. Takayama and T. Ito, *Chem. Lett.*, 2004, **33**, 1624–1625.
- 34 B. K. Breedlove, R. kandel, H. M. Ahsan and M. Yamashita, *Dalton Trans.*, 2014, **43**, 7683–7686.
- 35 H. E. Toma and K. Araki, *Coord. Chem. Rev.*, 2000, **196**, 307–329.
- 36 A. H. Reath, J. W. Ziller, C. Tsay, A. J. Ryan and Y. Yang, *Inorg. Chem.*, 2017, **56**, 3713–3718.
- 37 A. Mori, T. Suzuki, Y. Sunatsuki, A. Kobayashi, M. Kato, M. Kojima and K. Nakajima, *Eur. J. Inorg. Chem.*, 2014, 186–197.
- 38 A. Mori, T. Suzuki, Y. Sunatsuki, M. Kojima and K. Nakajima, *Bull. Soc. Jpn.*, 2015, **88**, 186–197.
- 39 C. Costentin, M. Robert and J. M. Saveant, *Chem. Soc. Rev.*, 2013, **42**, 2423–2436.
- 40 J. D. Cope, N. P. Liyanage, P. J. Kelley, J. A. Denny, E. J. Valente, C. E. webster, J. H. Delcamp, and T. K. Hollis, *Chem. Comm.*, 2017, **53**, 9442–9445.
- 41 J. D. Froehlich and C. P. Kubiak, *Inorg. Chem.*, 2012, **57**, 3932–3934.
- 42 D. C. Lacy, C. C. L. McCrory and J. C. Peters, *Inorg. Chem.*, 2014, **53**, 4980–4988.
- 43 D. C. Grills, Y. Matsubara, Y. Kuwahara, S. R. Golisz, D. A. Kurtz and B. A. Mello, *J. Phys. Chem. Lett.*, 2014, **5**, 2033–2038.
- 44 C. Riplinger, M. D. Sampson, A. M. Ritzmann, C. P. Kubiak and E. A. Carter, *J. Am. Chem. Soc.*, 2014, **136**, 16285–16298.

Attaching a redox-active metal complex to a CO<sub>2</sub> reduction electrocatalyst improves the overpotential and turnover frequency towards the reduction of CO<sub>2</sub> to CO.

